energies

MDPI

Article

Geochemical Characteristics of Coal in the Taiyuan Formation in the Center and North of the Xishan Coalfield

Gang Wang [1,*], Yong Qin [2] and Yiwei Xie [3]

[1] College of Architecture & Civil Engineering, Shangqiu Normal University, Shangqiu 476000, China
[2] Key Laboratory of Coalbed Methane Resources and Reservoir Formation Process of the Ministry of Education, China University of Mining and Technology, Xuzhou 221116, China
[3] Geology Section of the Xi Shan Coal Electricity Group, Taiyuan 030053, China
* Correspondence: wgkdwb@163.com; Tel.: +86-370-2591111

Abstract: The Xishan coalfield is an important coking coal-producing area in China. The No. 8 and No. 9 coals of the Taiyuan formation were sampled and tested from nine mines in the center and north of the Xishan coalfield, and the coal's quality characteristics, element occurrence characteristics, enrichment characteristics, and sedimentary environment characteristics were analyzed to provide a foundation for clean and efficient coal utilization and identification of associated coal resources. The results obtained from the experiment show that Li in No. 8 coal is the enrichment element. The enrichment coefficient of the U element of ML8 is 13.78, which is close to the industrial index of recycling. The enrichment hazardous elements are Cu, Mo, Cd of ML8, Mo of DQ8, and Th of ZCD8. Along with *K* value and Sr/Ba ratio, seawater has a greater influence on the south of No. 8 coal than on the north and on the east of No. 9 coal than on the west. No. 8 coal (except ML8) was formed under an oxidation environment based on the U/Th, Ni/Co, and V/Cr ratios. The oxidation or suboxic to the dysoxic environment resulted in the formation of No. 9 coal. Based on the Al_2O_3/TiO_2 ratio, the sediments of No. 8 and No. 9 coals are mainly from felsic volcanic rocks.

Keywords: Xishan coalfield; Taiyuan formation; elements; geochemistry; sedimentary environment

check for updates

Citation: Wang, G.; Qin, Y.; Xie, Y. Geochemical Characteristics of Coal in the Taiyuan Formation in the Center and North of the Xishan Coalfield. *Energies* **2022**, *15*, 8025. https://doi.org/10.3390/en15218025

Academic Editor: Manoj Khandelwal

Received: 1 October 2022
Accepted: 26 October 2022
Published: 28 October 2022

Publisher's Note: MDPI stays neutral with regard to jurisdictional claims in published maps and institutional affiliations.

Copyright: © 2022 by the authors. Licensee MDPI, Basel, Switzerland. This article is an open access article distributed under the terms and conditions of the Creative Commons Attribution (CC BY) license (https://creativecommons.org/licenses/by/4.0/).

1. Introduction

China has abundant coal resources and is the world's largest producer and consumer of coal [1]. China's coal consumption accounted for 57.7% of total primary energy consumption in 2019. Coal has occupied a dominant position for a long time. While the use of coal resources promotes economic development, serious environmental issues arise due to air pollutants, particulates, and coal-fired products [2–5]. Coal contains both major and trace elements, each of which have a different affinity for organic matter and inorganic minerals [6]. The environmental effect, sedimentary environment, and sediment source of coal can be understood through the study of the element geochemistry of coal [7], and three types of rare earth resources and hazardous trace elements associated with coal seams have been discovered, providing a theoretical basis for efficient and clean coal utilization [8,9].

The Xishan coalfield is one of the six largest coalfields in China's Shanxi Province. There are various types of coal, ranging from fat coal to anthracite. It is an important coking coal-producing region in China. The Xishan coalfield is 75-km long from north to south and 30-km long from east to west, with a total area of 1885 km^2 [10]. Some well fields in the Xishan coalfield have the potential mineralization of associated lithium and gallium. The rare earth elements related to coal in the Shanxi formation of the Xishan coalfield have industrial development and utilization values [11]. Many studies have been conducted to investigate the occurrence state, enrichment mechanism, and coal-forming environment of trace elements and rare earth elements in No. 8 coal [12–16]. The Malan well field has reached the minimum mining grade of lithium in coal. Lithium content in coal mainly occurs in inorganic minerals and has a high positive correlation with coal ash, gallium, and

thorium [17]. Gallium in the lower coal seam of the Shanxi formation in the Xingjiashe well field and No. 8 coal gangue of the Malan well field is close to the boundary grade of gallium in coal and gangue, both of which have potential industrial values [10].

Previous researchers conducted detailed studies on the trace elements and rare earth elements occurring in the coal gangue of the Duerping, Malan, and Dongqu well fields to investigate the geochemical characteristics of the elements in the gangue and provide a theoretical basis for gangue pollution control [12,18–20]. Sc, V, Cr, Ga, Rb, U, Nb, Cd, and Ta are enriched in the gangue of the Duerping well field, and rare earth elements are primarily enriched in clay minerals, such as kaolinite. The hazardous trace elements, such as Cr, Ni, and Cu, present in No. 2 coal gangue of the Malan well field, mainly occur in kaolinite with high crystallinity, which is controlled by kaolinite and quartz. The amount of enriched trace elements in the Shanxi formation exceed that in the Taiyuan formation. The Shanxi formation is a typical continental sedimentary environment with an oxidation environment. The Taiyuan formation is a typical marine and transitional sedimentary environment with an anoxic and reduction environment.

Although several previous studies have discussed the geochemical characteristics of coal seam and gangue, overall sampling is limited and research on the overall distribution of various elements and the regional change in coal seam sedimentary environment is scarce. Therefore, understanding the specific area of element enrichment and the changing trend of the sedimentary environment is impossible. Therefore, in this study, the No. 8 and No. 9 coals of the Taiyuan formation from nine mines in the center and north of the Xishan coalfield were sampled and tested, and the coal's quality characteristics, element occurrence characteristics, enrichment characteristics, and sedimentary environment characteristics were analyzed to provide a foundation for clean and efficient coal utilization and identification of associated coal resources.

2. Geological Background

2.1. Tectonic

The study area is located in the center and north of the Xishan coalfield, which is connected to the Fenhe structural basin in the southeast and belongs to the central area of North China Craton [21]. The coalfield is generally small in the south and large in the north, indicating a "torch–shaped" compound syncline structure (Figure 1). After the coal-accumulating Carboniferous and Permian periods, the Xishan coal field underwent crustal uplift movement during the Indosinian period, strong compression movement during the Yanshanian period, dominated by folds, along with faults as well as magmatic rock intrusion, and tectonic movement in the Himalayan period, dominated by NEE faults, forming the current structural pattern of the Xishan coalfield.

The SN and NEE structures dominate the Xishan coalfield (Figure 1). Large SN-trending folds (such as the Malan syncline and the Shuiyuguan syncline) run through the coalfield's center and west, forming a syncline structure with a steep and gentle slope along the west and east, respectively. The SN faults mainly comprise coalfield marginal faults located in the west. The east wing of the syncline is cut into several rectangular blocks, and the NE as well as NNE faults are distributed in a belt.

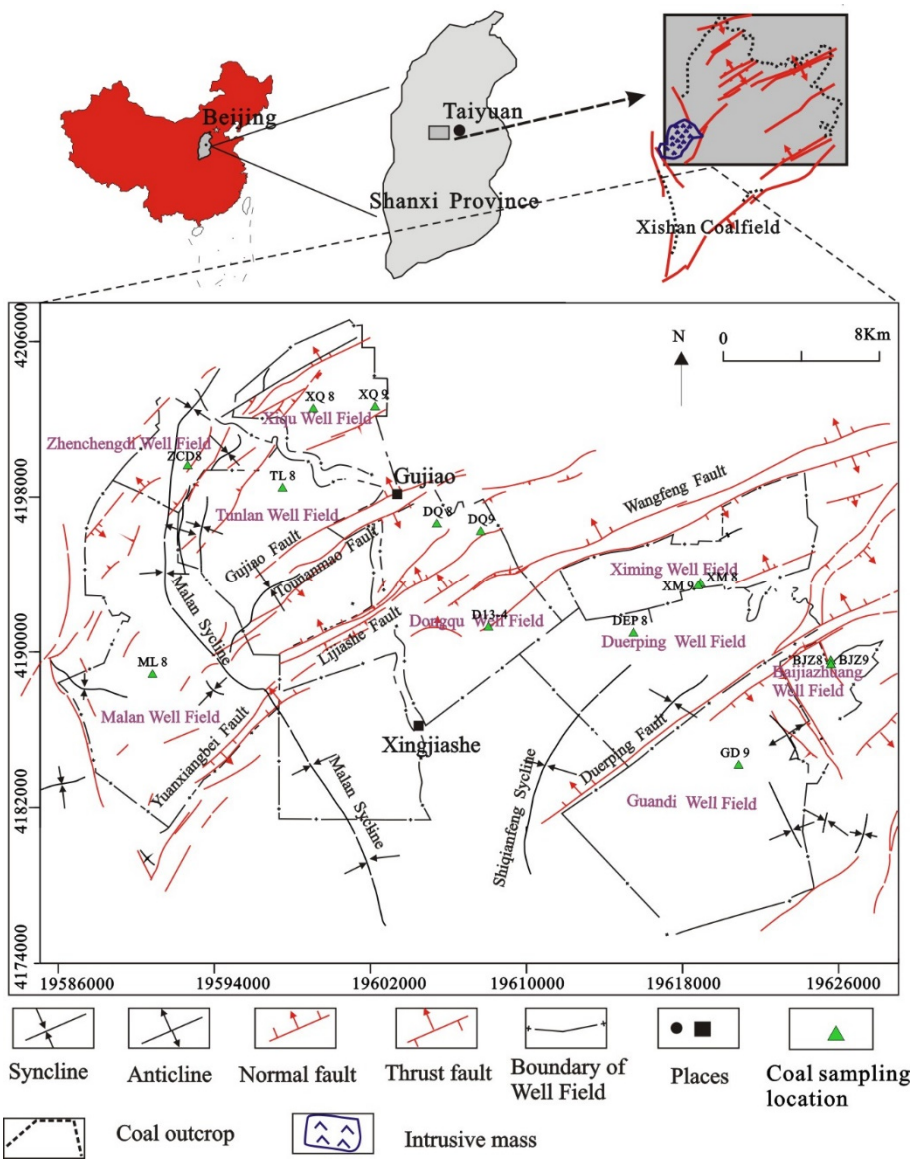

Figure 1. Structural outlines and distribution of sampling points in the study area.

2.2. Coal-Bearing Strata

The main coal-bearing strata in this area are the late Carboniferous Taiyuan formation and the early Permian Shanxi formation. The Taiyuan formation is continuously deposited on the underlying strata, which is divided into the following three lithologic sections: Dongdayao, Maoergou, and Jinci. The thickness of the lower Jinci section ranges from 15.38 to 44.79 m, with 2 to 3 coal seams. The bottom marker layer is a white medium coarse quartz sandstone, which is called Jinci sandstone (K_1). Maoergou section thickness in the middle ranges from 27.60 to 40.20 m, with an average of 34.95 m. It comprises carbonate rock; clastic rock mixed with black mudstone; and No. 8, No. 9, and No. 10 coals. The upper Dongdayao section's thickness ranges from 26.60 to 51.10 m, with an average of 45.10 m. It mainly comprises gray–white sandstone with two layers of unstable coal seams. The bottom layer comprises No. 7 coal, and the roof comprises Xiedao limestone (L_4). The top layer comprises No. 6 coal, and the roof comprises Dongdayao limestone (L_5) [22] (Figure 2).

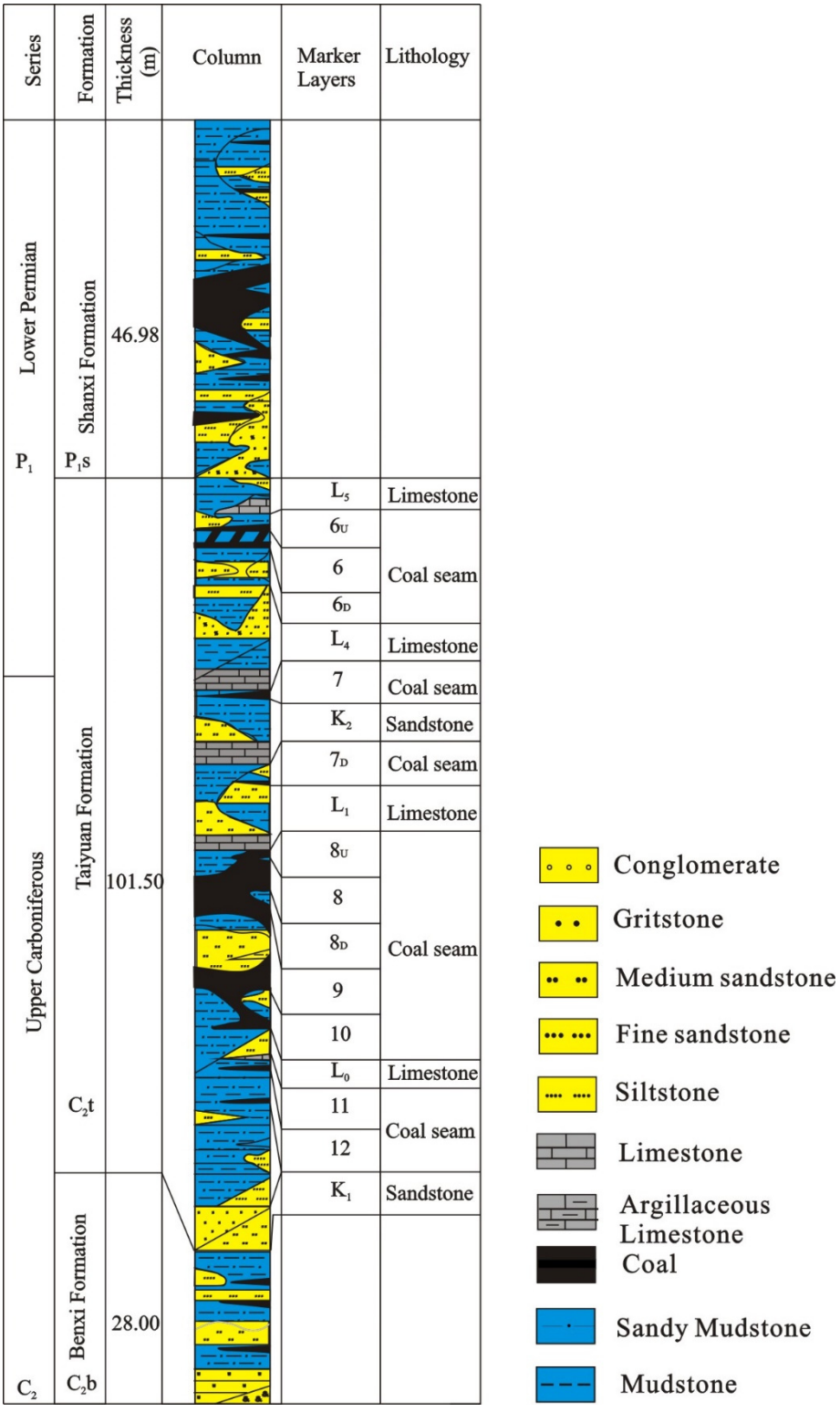

Figure 2. Comprehensive histogram of coal-bearing strata.

The No. 8 coal developed steadily in the study area. The buried depth varies between 357.01 and 906.20 m, with an average of 639.70 m. The thickness ranges from 1.5 to 5.0 m. Limestone, marlstone, mudstone, and sandstone dominate the roof's lithology. The No. 9 coal has a high degree of stability. The buried depth ranges from 363.45 to 915.15 m, with an average of 644.44 m. The thickness ranges from 0.65 to 4.70 m, with an average of 1.96 m. The roof mainly comprises sandstone, mudstone, and carbonaceous shale. The distance

between No. 8 and No. 9 coals ranges from 0.86 to 26.29 m, with an average of 11.37 m, indicating that they are relatively close [16].

3. Sampling and Experiment

The samples were collected from No. 8 and No. 9 coals of nine coal mines in the middle and north of the Xishan coalfield according to the national standards of the People's Republic of China (GB482-2008) (Figure 1). Because the coal seam is thick, samples were collected from the thick coal seam's midpoint. The samples were prepared according to national standards of the People's Republic of China (GB/T474-1996). Natural ventilation was used to dry the collected samples. The samples were crushed into 20-mesh, 80-mesh, and 200-mesh sizes according to GB474-2008 and prepared for observation of coal macerals as well as vitrinite reflectance measurement, proximate analysis, and determination of associated elements, respectively. The proximate analysis was performed at the Key Laboratory of Coalbed Methane Resources and Reservoir Formation Process of the Ministry of Education according to the GB/T212-2008. The total sulfur content in coal was determined using GB/T214-2007, and the test was completed at the Jiangsu Design Institute of Geology for Mineral Resources. The maceral classification in this study is based on Taylor et al. [23] and the ICCP System 1994 [24,25]. The elemental analysis was completed at the Regional Geological Survey Institute in Hebei Province. The major elements of the coal samples were determined via X-ray fluorescence spectrometry (Axios^{max}) according to GB/T 14506.14-2010 and GB/T 14506.28-2010. ICP–MS (X series2) was used to determine the trace elements and rare earth elements per GB/T 14506.30-2010 [26].

4. Results

4.1. Coal's Quality

The macrolithotypes of No. 8 coal are mainly semibright coal and bright coal. The maximum vitrinite reflectance ranges from 1.14% to 2.30%, with an average of 1.74%. Coal macerals are mainly vitrinite and inertinite. Vitrinite content ranges from 63.70% to 87.16%, with an average of 74.83%. The inertinite content ranges from 5.67% to 34.13%, with an average of 20.83%. The mineral composition ranges from 0% to 9.65%, with an average of 3.58%. The yield of volatile matter when air dried ranges from 11.71% to 26.39%, with an average of 16.84%. The ash yield ranges from 3.70% to 11.32%, with an average of 7.39%. Total sulfur content ranges from 1.54% to 4.74%, with an average of 2.58% (Table 1).

The macrolithotype of No. 9 coal mainly comprises semibright coal, and the maximum vitrinite reflectance ranges from 1.93% to 2.39%, with an average of 2.18%. Coal macerals are primarily vitrinite and inertinite. Vitrinite content ranges from 59.00% to 89.57%, with an average of 76.41%. The inertinite content ranges from 8.38% to 38.00%, with an average of 20.78%. Mineral content ranges from 0% to 5.60%, with an average of 2.39%. The yield of volatile matter when air dried ranges from 11.14% to 17.51%, with an average of 13.61%. The ash yield ranges from 7.58% to 14.73%, with an average of 10.02%. Total sulfur content ranges from 0.85% to 1.59%, with an average of 1.05% (Table 1).

According to national standards of the People's Republic of China (GB/T 15224.1-2004, GB/T 15224.2-2004), when the ash yield is less than 10%, the coal is ultralow ash coal and when the ash yield is 10.01–16.00%, it is low ash coal. Therefore, most No. 8 and No. 9 coal samples are ultralow ash coal and some coal samples are low ash coal. The vast majority of No. 8 coal is medium–high sulfur coal. The total sulfur content of ML8 and DEP8 is greater than 3%, indicating that the coal is high in sulfur. The majority of No. 9 coal is low sulfur coal, with some samples being medium–high sulfur coal. The coal ash yield of No. 8 coal decreases gradually from west to east, whereas that of No. 9 coal decreases gradually from north to south (Figure 3). The distribution of total sulfur in No. 8 coal is opposite to that of ash yield, with an increasing trend from northwest to southeast. The total sulfur content of No. 9 coal decreases from north to south, similar to the ash yield (Figure 4).

Table 1. Basic features of coal samples in the Gujiao Block.

Coal	Samples	Well Field	Macrolithotype	$R_{o,max}$ (%)	Coal Macerals (%)				Proximate Analysis (%)				Ultimate Analyses (%)				
					V	*I*	*E*	*M*	M_{ad}	A_d	V_{daf}	FC_d	C_{daf}	H_{daf}	O_{daf}	N_{daf}	$S_{t,d}$
8	BJZ8	Baijiazhuang	Bright coal	2.25	78.56	20.87	0.57	0	1.45	3.7	11.71	85.02	-	-	-	-	-
	D13-4	Dongqu	Semibright coal	2.04	86.67	5.67	0.33	7.33	0.8	6.98	14.3	79.72	90	4.29	2.71	1.32	1.56
	DEP8	Duerping	Bright coal	2.3	87.16	9	1.72	2.11	1.09	8.36	13.02	79.72	91.11	4.17	1.9	1.16	4.74
	DQ8	Dongqu	Semibright coal	1.74	74.92	20.2	0.65	4.23	1.16	10.26	16.8	74.67	-	-	-	-	-
	ML8	Malan	Semibright coal	1.25	68.14	25.66	0.88	5.31	0.59	9.36	22.19	69.21	89.45	4.91	4.46	1.5	3.46
	TL8	Tunlan	Semidull coal	1.43	63.7	33.7	0.74	1.85	0.79	6	17.2	77.19	89.74	4.78	2.81	1.29	1.54
	XM8	Ximing	Semibright coal	2.05	83.91	15.13	0.96	0	0.99	5.13	12.35	83.15	91.13	4.08	1.76	1.43	2.17
	XQ8	Xiqu	Semibright coal	1.47	63.82	34.13	0.34	1.71	0.9	5.36	17.57	77.28	89.62	4.81	2.55	1.33	2.77
	ZCD8	Zhenchengdi	Bright coal	1.14	66.56	23.15	0.64	9.65	0.51	11.32	26.39	64.91	89.13	4.94	3.03	1.33	1.79
9	BJZ9	Baijiazhuang	Semibright coal	2.1	68.73	25.29	0.39	5.6	1.25	10.2	12.22	78.83	-	-	-	-	-
	D13-4	Dongqu	Semibright coal	2.26	81	17	1	1	1.08	8.17	13.21	79.7	91.36	3.92	2.99	1.12	0.85
	DQ9	Dongqu	Semibright coal	2.18	83.3	12.9	0.19	3.61	1.03	14.73	15.01	72.47	-	-	-	-	-
	GD9	Guandi	Semibright coal	2.39	59	38	0	3	1.28	7.58	11.14	82.13	91.29	3.93	3.23	1.55	0.86
	XM9	Ximing	Semibright coal	2.24	89.57	8.38	1.12	1.12	1.09	10.37	12.58	78.35	90.55	3.92	2.29	1.36	0.89
	XQ9	Xiqu	Semibright coal	1.93	76.88	23.12	0	0	0.86	9.08	17.51	75.01	89.75	4.7	3.08	1.42	1.59

$R_{o,max}$ mean maximum vitrinite reflectance in oil. *V*, *I*, and *E* represent the volume percentages of vitrinite, inertinite and liptinite in the coal maceral composition, respectively. *M* is the volume percentage of minerals on a dry basis. V_{daf}, M_{ad}, and A_{ad} represent the volatile yield, moisture content and ash yield respectively. C, carbon; H, hydrogen; N, nitrogen; S_t, total sulfur; ad, air-dry basis; d, dry basis; daf, dry and ash-free basis.

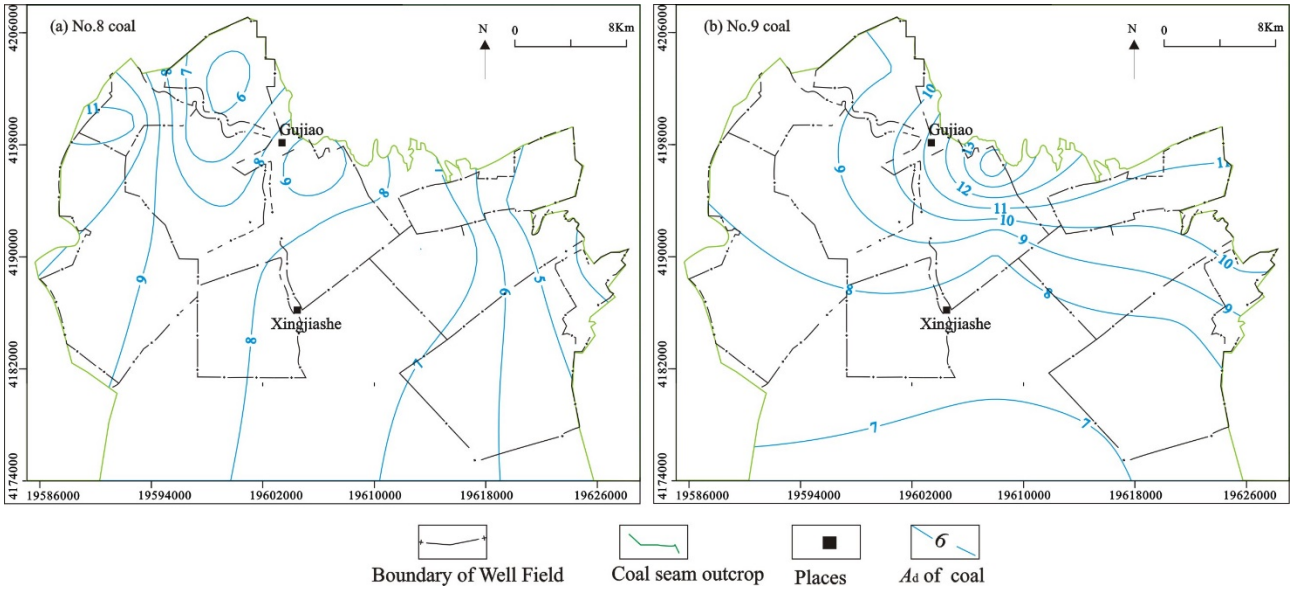

Figure 3. Contour map of coal ash yield.

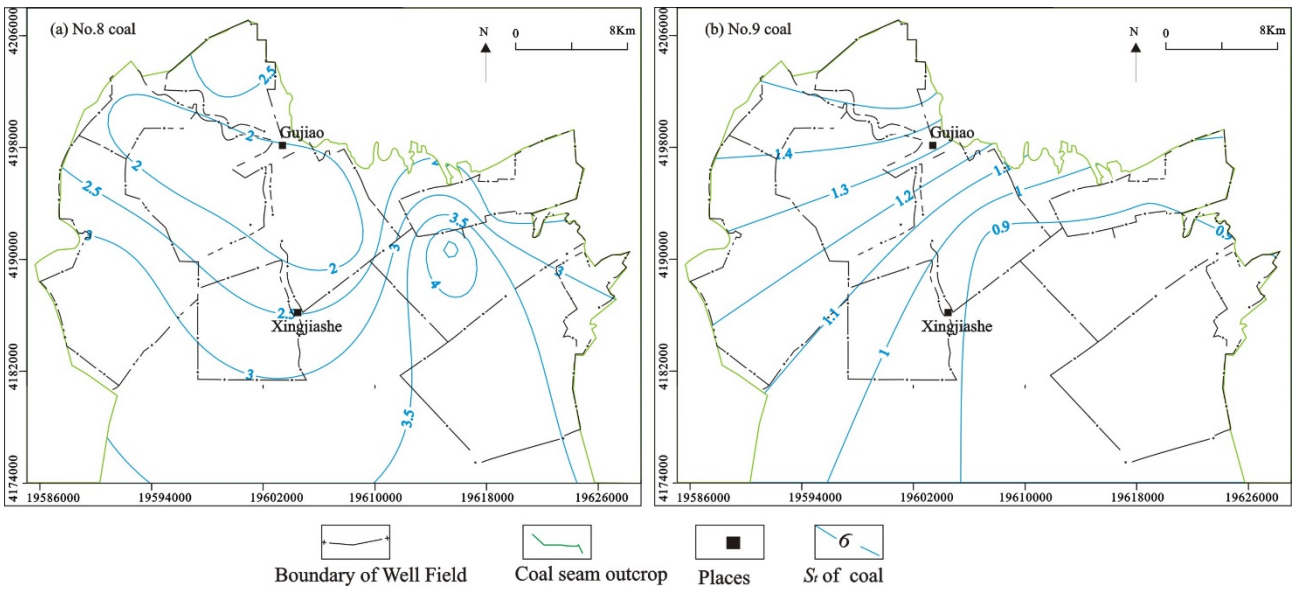

Figure 4. Contour map of total sulfur in coal seam.

4.2. Major Element

Si and Al are the most abundant elements in the coal ash of No. 8 and No. 9 coals, followed by Ca and Fe (Table 2; Figure 5). The Si content of No. 8 coal ranges from 0.77% to 6.29%, with an average of 2.67%. The Al content ranges from 0.73% to 5.80%, with an average of 2.52%. ZCD8 and DQ8 have the highest Si and Al content, followed by ML8, XQ8, TL8, DEP8, XM8, and BJZ8. The Si content of No. 9 coal ranges from 1.35% to 3.44%, with an average of 2.24%. The Al content ranges from 1.20% to 3.27%, with an average of 2.14%. The content of Si and Al in DQ9 is the highest, and the content of GD9 and BJZ9 is the lowest. The Si and Al content in No. 9 coal is slightly lower than that in No. 8 coal but the general distribution trend, which decreases from west to east, is similar to that of No. 8 coal.

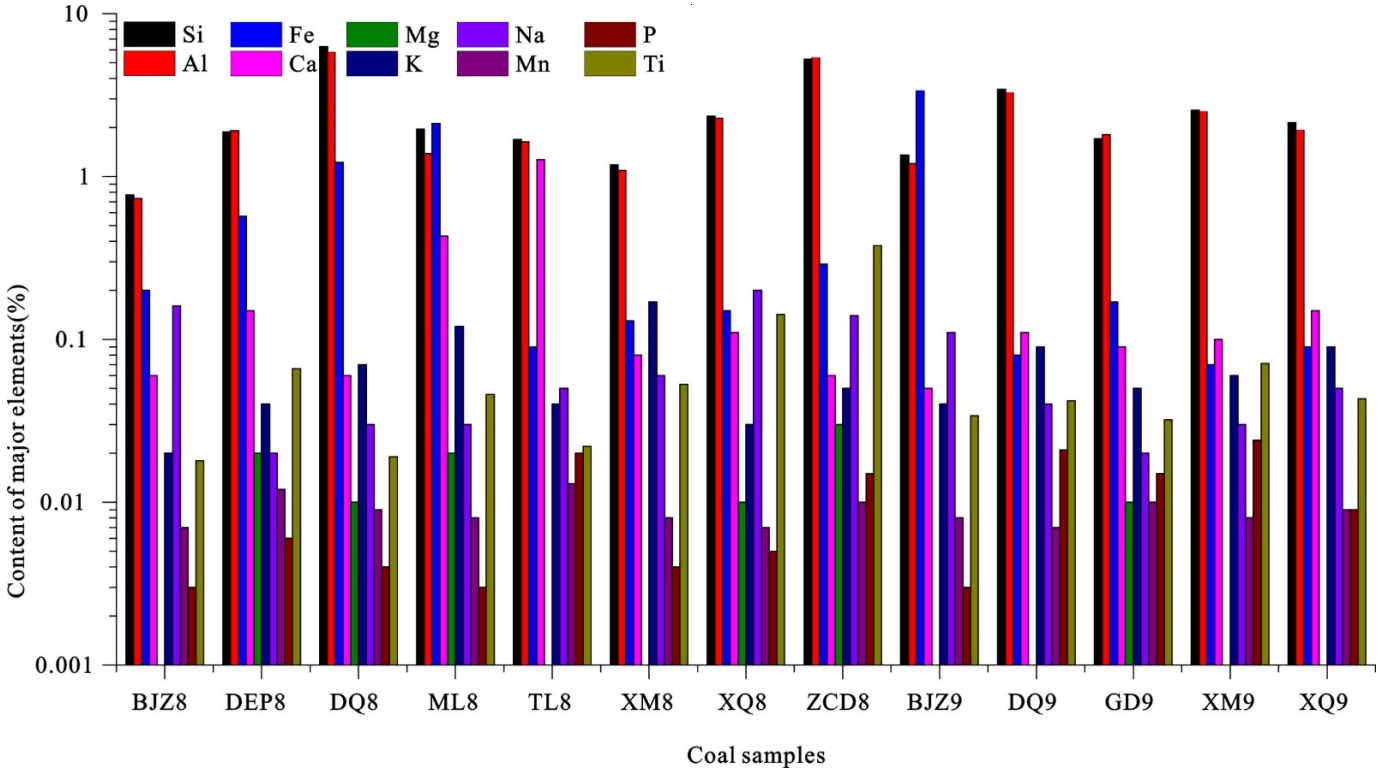

Figure 5. Comparison of major element content of coal sample.

Table 2. Major element analysis of coal sample.

Samples	Major Element (%)										*K*	*X*	*Y*
	Si	Al	Fe	Ca	Mg	K	Na	Mn	P	Ti			
BJZ8	0.77	0.73	0.20	0.06	0.00	0.02	0.16	0.007	0.003	0.018	0.12	1.19	47.22
DEP8	1.88	1.91	0.57	0.15	0.02	0.04	0.02	0.012	0.006	0.066	0.14	1.12	32.94
DQ8	6.29	5.80	1.22	0.06	0.01	0.07	0.03	0.009	0.004	0.019	0.08	1.23	354.47
ML8	1.96	1.38	2.12	0.43	0.02	0.12	0.03	0.008	0.003	0.046	0.54	1.61	34.25
TL8	1.69	1.63	0.09	1.27	0.00	0.04	0.05	0.013	0.020	0.022	0.28	1.17	85.07
XM8	1.18	1.09	0.13	0.08	0.00	0.17	0.06	0.008	0.004	0.053	0.06	1.22	23.19
XQ8	2.34	2.28	0.15	0.11	0.01	0.03	0.20	0.007	0.005	0.142	0.04	1.16	18.19
ZCD8	5.25	5.36	0.29	0.06	0.03	0.05	0.14	0.010	0.015	0.377	0.03	1.11	16.09
Minimum	0.77	0.73	0.09	0.06	0.00	0.02	0.02	0.01	0.00	0.02	0.03	1.11	16.09
Maximum	6.29	5.80	2.12	1.27	0.03	0.17	0.20	0.01	0.02	0.38	0.54	1.61	354.47
Average	2.67	2.52	0.60	0.28	0.01	0.07	0.09	0.01	0.01	0.09	0.16	1.23	76.43
BJZ9	1.35	1.20	3.36	0.05	0.00	0.04	0.11	0.008	0.003	0.034	0.95	1.28	39.99
DQ9	3.44	3.27	0.08	0.11	0.00	0.09	0.04	0.007	0.021	0.042	0.02	1.19	88.64
GD9	1.71	1.81	0.17	0.09	0.01	0.05	0.02	0.010	0.015	0.032	0.06	1.07	63.94
XM9	2.55	2.50	0.07	0.10	0.00	0.06	0.03	0.008	0.024	0.071	0.02	1.16	39.79
XQ9	2.14	1.92	0.09	0.15	0.00	0.09	0.05	0.009	0.009	0.043	0.04	1.26	50.85
Minimum	1.35	1.20	0.07	0.05	0.00	0.04	0.02	0.01	0.00	0.03	0.02	1.07	39.79
Maximum	3.44	3.27	3.36	0.15	0.01	0.09	0.11	0.01	0.02	0.07	0.95	1.28	88.64
Average	2.24	2.14	0.76	0.10	0.00	0.07	0.05	0.01	0.01	0.04	0.2	1.19	56.64

$K = (Fe_2O_3 + CaO + MgO)/(SiO_2 + Al_2O_3)$; $X = SiO_2/Al_2O_3$; $Y = Al_2O_3/TiO_2$.

The correlation coefficient between Si and Al in No. 8 and No. 9 coal is 0.99, and their correlation coefficient with ash exceeds 0.75. Therefore, they are the main components of ash. No. 8 coal has a SiO_2/Al_2O_3 ratio ranging from 1.11 to 1.61, with an average of 1.23. The SiO_2/Al_2O_3 ratio of No. 9 coal ranges from 1.07 to 1.28, with an average of 1.19, slightly lower than that of No. 8 coal. According to previous research, the minerals in coal

are primarily clay minerals dominated by kaolinite, with some samples containing a certain amount of quartz. The average SiO_2/Al_2O_3 ratio of the two coal seams is higher than the kaolinite ratio (1.18), indicating the presence of free SiO_2, which is consistent with previous studies [12,13,27,28].

The Fe content of No. 8 coal is higher in the Malan well field and Dongqu well field. In the Baijiazhuang well field, the Fe content of No. 9 coal is higher. The correlation coefficient between Fe and total sulfur in No. 8 coal is 0.47, which may be attributed to the presence of pyrite in coal [12]. Furthermore, there is a positive correlation between total sulfur and Mg in No. 8 coal. The positive correlation between total sulfur and Ca, K, and Na of No. 9 coal is greater than 0.95 (Tables 3 and 4).

Table 3. Correlation coefficient analysis of major elements of No. 8 coal.

Correlation Coefficient	Si	Al	Fe	Ca	Mg	K	Na	Mn	P	Ti	A_d	St	C
Si	1.00	0.99	0.25	−0.27	0.54	−0.12	−0.09	0.03	0.46	0.46	0.80	−0.29	−0.63
Al		1.00	0.14	−0.28	0.56	−0.18	−0.03	0.07	0.21	0.53	0.78	−0.30	−0.55
Fe			1.00	−0.04	0.32	−0.18	−0.52	−0.21	−0.38	−0.23	0.55	0.47	−0.24
Ca				1.00	−0.22	−0.10	−0.33	0.64	0.71	−0.29	−0.13	−0.36	−0.23
Mg					1.00	−0.18	−0.14	0.31	0.22	0.68	0.86	0.33	−0.31
K						1.00	−0.49	−0.27	−0.33	−0.21	0.04	−0.08	0.41
Na							1.00	−0.48	−0.04	0.47	−0.38	−0.37	−0.51
Mn								1.00	0.77	0.02	0.23	0.01	0.15
P									1.00	0.37	0.18	−0.61	−0.40
Ti										1.00	0.49	−0.31	−0.52
Ad											1.00	0.19	−0.45
St												1.00	0.42
C													1.00

Table 4. Correlation coefficient analysis of major elements of No. 9 coal.

Correlation Coefficient	Si	Al	Fe	Ca	Mg	K	Na	Mn	P	Ti	Ad	St	C
Si	1.00	0.99	−0.63	0.52	−0.47	0.72	−0.51	−0.70	0.77	0.42	0.81	0.05	−0.49
Al		1.00	−0.69	0.49	−0.34	0.65	−0.61	−0.62	0.85	0.43	0.75	−0.33	−0.13
Fe			1.00	−0.81	−0.08	−0.62	0.96	−0.09	−0.74	−0.39	−0.06	−0.39	0.76
Ca				1.00	−0.27	0.87	−0.61	−0.04	0.33	0.26	0.06	0.99	−0.95
Mg					1.00	−0.46	−0.31	0.78	−0.10	−0.51	−0.61	−0.53	0.85
K						1.00	−0.38	−0.46	0.27	0.06	0.48	1.00	−0.93
Na							1.00	−0.24	−0.78	−0.36	0.06	0.96	−0.98
Mn								1.00	−0.26	−0.22	−0.96	−0.34	0.73
P									1.00	0.68	0.41	−0.76	0.39
Ti										1.00	0.16	−0.22	−0.25
Ad											1.00	0.20	−0.60
St												1.00	−0.90
C													1.00

Calcite is the main carrier of Ca in coal. The marine animal fossils, such as brachiopods, lamellibranchs, foraminifera, echinoderms, and their fragments, found in the late Carboniferous coal of the Xishan coalfield, are a source of Ca [29]. The Ca of No. 8 coal has a good correlation with Mn (r = 0.64) and P (r = 0.71) but is negatively correlated with other elements. The Ca content in No. 9 coal is positively correlated with Si, Al, K, and S_t and negatively correlated with Fe, Na, and C. Ti has a strong positive correlation with Si, Al, and P.

4.3. Trace Element

The enrichment coefficient is defined in this study as the ratio of trace element content of coal samples in the study area to Chinese coal. When the ratio is less than 0.5, 0.5–2, 2–5, 5–10, and greater than 10, it indicates depletion, similarity, slight enrichment, enrichment, and considerable enrichment, respectively [9,30]. Depleted elements include Co, Ni, Rb, Sb, Cs, Ba, Hf, Ta, W, Ti, Bi, P, and B of No. 8 coal and V, Co, Ni, Cu, Rb, Nb, Mo, Sb, Cs, Ba, Hf, Ta, W, Tl, Bi, P, and B of No. 9 coal.

Li and U are minor enrichment elements in No. 8 coal. The Li content in DQ8 and ZCD8 are relatively high, with enrichment coefficients of 3.42 and 8.52, respectively (Tables 5 and 6; Figure 6); Li content decreases from northwest to southeast, with a relatively fast decrease in the northwest. According to Sun et al. [31], the recovery and utilization index of lithium in raw coal is 120 μg/g. Therefore, the Zhenchengdi well field in the study area's northwest and some areas of the Malan well field can consider the recovery and utilization of Li element in coal (Figure 7). Lithium content in coal gangue or close to coal gangue, the roof, and the floor is relatively high, and it is highly positively correlated with ash, gallium, and thorium elements. The most likely carriers for lithium adsorption are clay minerals [17].

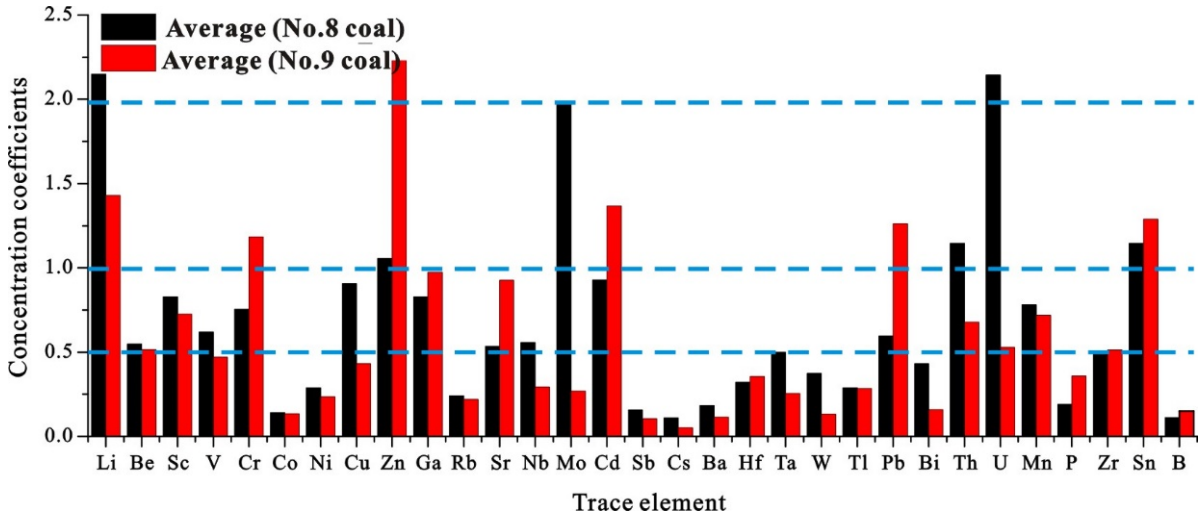

Figure 6. Average enrichment coefficient of trace elements in a coal sample.

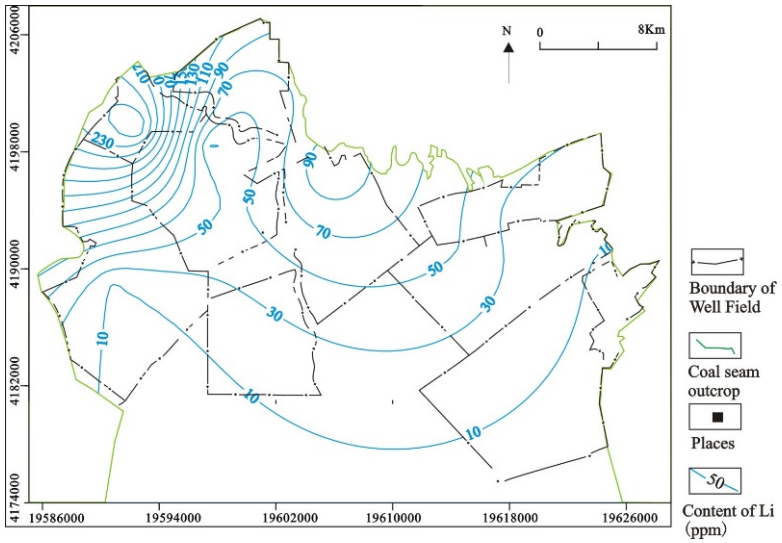

Figure 7. Li content distribution of No. 8 coal.

Table 5. Trace elements content in coal samples (μg/g).

Samples	BJZ8	DEP8	DQ8	ML8	TL8	XM8	XQ8	ZCD8	Average (No. 8 Coal)	BJZ9	DQ9	GD9	XM9	XQ9	Average (No. 9 Coal)	Chinese Coal [a]	North China Coal [b]	Average (No. 8 Coal)/Average (No. 9 Coal)
Li	6.66	46.9	109	7.83	28.2	17.2	60.4	271	68.32	14.9	76.7	52.2	59.7	23.7	45.5	31.8	43.91	1.50
Be	0.34	1.18	1.54	2.95	0.59	0.54	0.71	1.42	1.16	1.16	0.64	0.68	1.06	1.89	1.1	2.11	2.05	1.06
Sc	1.69	3.83	3.25	2.42	2.66	2.14	3.59	9.43	3.63	2.27	4.04	2.98	3.05	3.54	3.2	4.38	6.32	1.14
V	11.1	27.3	12.4	51.2	13.2	11.7	16.1	30.8	21.73	13.0	20.2	17.3	13.7	18.2	16.5	35.1	31.3	1.32
Cr	7.54	11.3	7.96	19.4	8.25	6.94	10.4	21.1	11.62	58.7	8.94	7.26	7.84	8.43	18.2	15.4	14.98	0.64
Co	0.40	2.08	0.92	1.23	1.61	0.26	1.05	0.42	0.99	2.01	0.39	0.80	0.80	0.75	0.9	7.08	4.06	1.05
Ni	1.33	2.70	3.71	15.1	4.35	1.05	1.75	1.67	3.95	7.63	2.32	1.70	1.74	2.66	3.2	13.7	6.65	1.23
Cu	5.82	4.82	20.8	36.3	10.7	2.86	13.0	32.8	15.88	14.5	2.85	5.50	8.86	6.19	7.6	17.5	10.28	2.10
Zn	55.2	117	68.5	17.8	22.2	52.9	7.6	8.92	43.75	78.6	54.6	101	103	124	92.3	41.4	25	0.47
Ga	1.08	5.19	3.36	7.51	11.3	1.78	4.59	8.62	5.43	5.67	9.11	4.13	5.07	7.89	6.4	6.55	12.5	0.85
Rb	0.6	1.0	2.5	4.2	1.2	5.7	1.1	1.5	2.23	1.3	2.0	1.3	2.1	3.5	2.0	9.25	1.59	1.09
Sr	40.9	46.5	20.5	82.9	230	38.8	56.8	82.7	74.86	21.1	115	136	220	158	129.9	140	192	0.58
Nb	0.33	3.46	1.78	2.72	2.34	2.36	5.90	23.3	5.27	1.87	1.48	2.80	4.21	3.46	2.8	9.44	6.87	1.91
Mo	0.28	0.45	13.6	28.9	1.24	0.38	1.32	2.87	6.12	1.29	0.57	0.57	0.55	1.16	0.8	3.08	2.39	7.38
Cd	0.21	0.42	0.27	0.58	0.12	0.17	0.026	0.061	0.23	0.42	0.21	0.35	0.25	0.48	0.3	0.25	0.11	0.68
In	0.017	0.061	0.049	0.018	0.022	0.014	0.030	0.14	0.04	0.019	0.35	0.033	0.037	0.041	0.1	nd	nd	0.45
Sb	0.01	0.31	0.09	0.26	0.06	0.04	0.13	0.15	0.13	0.13	0.03	0.12	0.12	0.05	0.1	0.84	0.89	1.48
Cs	0.072	0.045	0.18	0.088	0.062	0.25	0.17	0.13	0.12	0.10	0.028	0.037	0.057	0.068	0.1	1.13	0.39	2.16
Ba	18.8	16.6	34.8	27.2	19.0	17.1	18.4	80.5	29.03	16.1	28.5	11.4	17.6	17.0	18.1	159	121.59	1.60
Hf	0.22	1.02	0.53	0.83	0.85	0.75	1.25	4.10	1.19	0.76	2.70	0.86	1.20	1.09	1.3	3.71	5.07	0.90
Ta	0.025	0.28	0.10	0.10	0.058	0.16	0.26	1.51	0.31	0.11	0.15	0.14	0.25	0.14	0.2	0.62	0.6	1.96
W	0.049	0.27	0.13	0.17	0.18	0.21	0.33	1.90	0.40	0.086	0.14	0.094	0.24	0.14	0.1	1.08	0.8	2.85
Tl	0.019	0.047	0.067	0.70	0.035	0.064	0.067	0.084	0.14	0.40	0.031	0.095	0.059	0.088	0.1	0.47	0.22	1.01
Pb	7.04	7.55	19.0	7.75	1.63	2.94	9.17	16.9	8.99	44.8	1.16	12.6	15.7	21.1	19.1	15.1	18.3	0.47
Bi	0.07	0.34	0.12	0.41	0.06	0.11	0.32	1.31	0.34	0.11	0.07	0.10	0.17	0.18	0.1	0.79	0.51	2.73
Th	0.65	5.40	1.61	2.89	1.64	3.50	5.06	32.75	6.69	2.17	7.50	2.69	4.17	3.28	4.0	5.84	7.56	1.69
U	0.20	1.22	0.93	33.5	0.70	0.65	1.00	3.49	5.21	0.63	1.75	1.49	1.02	1.52	1.3	2.43	3.26	4.06
Zr	7.33	36.4	20.8	39.6	31.3	24.9	46.1	157	45.39	26.5	91.9	33.6	39.6	38.7	46.0	90	188	1.09
Sn	2.74	2.48	1.93	1.98	1.63	2.69	3.73	2.18	2.42	1.54	3.81	1.41	1.95	4.90	2.7	2.11	4.47	0.53
B	4.43	6.74	3.90	2.63	4.31	8.84	10.7	5.41	5.87	8.66	8.24	8.22	4.70	9.83	7.9	53	nd	0.99

nd: no data; [a] From Dai et al. [32]; [b] From Ren et al. [33]; and Sun et al. [12].

Table 6. Enrichment coefficient of trace elements in coal samples compared with that in China.

Samples	BJZ8	DEP8	DQ8	ML8	TL8	XM8	XQ8	ZCD8	Average (No. 8 Coal)	BJZ9	DQ9	GD9	XM9	XQ9	Average (No. 9 Coal)
Li	0.21	1.47	3.42	0.25	0.89	0.54	1.90	8.52	2.15	0.47	2.41	1.64	1.88	0.75	1.43
Be	0.16	0.56	0.73	1.40	0.28	0.25	0.34	0.67	0.55	0.55	0.30	0.32	0.50	0.90	0.52
Sc	0.39	0.88	0.74	0.55	0.61	0.49	0.82	2.15	0.83	0.52	0.92	0.68	0.70	0.81	0.73
V	0.32	0.78	0.35	1.46	0.38	0.33	0.46	0.88	0.62	0.37	0.58	0.49	0.39	0.52	0.47
Cr	0.49	0.74	0.52	1.26	0.54	0.45	0.68	1.37	0.75	3.81	0.58	0.47	0.51	0.55	1.18
Co	0.06	0.29	0.13	0.17	0.23	0.04	0.15	0.06	0.14	0.28	0.06	0.11	0.11	0.11	0.13
Ni	0.10	0.20	0.27	1.10	0.32	0.08	0.13	0.12	0.29	0.56	0.17	0.12	0.13	0.19	0.23
Cu	0.33	0.28	1.19	2.08	0.61	0.16	0.74	1.87	0.91	0.83	0.16	0.31	0.51	0.35	0.43
Zn	1.33	2.82	1.65	0.43	0.54	1.28	0.18	0.22	1.06	1.90	1.32	2.45	2.48	3.00	2.23
Ga	0.16	0.79	0.51	1.15	1.73	0.27	0.70	1.32	0.83	0.87	1.39	0.63	0.77	1.21	0.97
Rb	0.07	0.11	0.27	0.45	0.13	0.62	0.12	0.17	0.24	0.14	0.21	0.14	0.23	0.37	0.22
Sr	0.29	0.33	0.15	0.59	1.64	0.28	0.41	0.59	0.53	0.15	0.82	0.97	1.57	1.13	0.93
Nb	0.04	0.37	0.19	0.29	0.25	0.25	0.63	2.46	0.56	0.20	0.16	0.30	0.45	0.37	0.29
Mo	0.09	0.15	4.41	9.38	0.40	0.12	0.43	0.93	1.99	0.42	0.18	0.18	0.18	0.38	0.27
Cd	0.84	1.66	1.09	2.32	0.47	0.69	0.11	0.24	0.93	1.67	0.84	1.40	1.00	1.94	1.37
In	-	-	-	-	-	-	-	-	-	-	-	-	-	-	-
Sb	0.02	0.37	0.10	0.31	0.07	0.05	0.15	0.18	0.16	0.16	0.04	0.14	0.14	0.05	0.11
Cs	0.06	0.04	0.16	0.08	0.05	0.22	0.15	0.11	0.11	0.09	0.02	0.03	0.05	0.06	0.05
Ba	0.12	0.10	0.22	0.17	0.12	0.11	0.12	0.51	0.18	0.10	0.18	0.07	0.11	0.11	0.11
Hf	0.06	0.28	0.14	0.22	0.23	0.20	0.34	1.11	0.32	0.20	0.73	0.23	0.32	0.29	0.36
Ta	0.04	0.44	0.16	0.16	0.09	0.25	0.41	2.43	0.50	0.18	0.23	0.22	0.40	0.23	0.25
W	0.05	0.25	0.12	0.16	0.17	0.19	0.30	1.76	0.37	0.08	0.13	0.09	0.22	0.13	0.13
Tl	0.04	0.10	0.14	1.50	0.07	0.14	0.14	0.18	0.29	0.84	0.07	0.20	0.13	0.19	0.29
Pb	0.47	0.50	1.26	0.51	0.11	0.19	0.61	1.12	0.60	2.97	0.08	0.84	1.04	1.39	1.26
Bi	0.09	0.42	0.15	0.52	0.08	0.14	0.40	1.66	0.43	0.14	0.09	0.13	0.21	0.22	0.16
Th	0.11	0.92	0.28	0.50	0.28	0.60	0.87	5.61	1.14	0.37	1.28	0.46	0.71	0.56	0.68
U	0.08	0.50	0.38	13.78	0.29	0.27	0.41	1.44	2.14	0.26	0.72	0.61	0.42	0.62	0.53
Mn	0.63	1.02	0.73	0.67	1.09	0.68	0.60	0.84	0.78	0.70	0.61	0.83	0.71	0.74	0.72
P	0.08	0.16	0.11	0.08	0.51	0.09	0.12	0.37	0.19	0.08	0.52	0.36	0.60	0.23	0.36
Zr	0.08	0.40	0.23	0.44	0.35	0.28	0.51	1.74	0.50	0.29	1.02	0.37	0.44	0.43	0.51
Sn	1.30	1.18	0.91	0.94	0.77	1.27	1.77	1.03	1.15	0.73	1.81	0.67	0.92	2.32	1.29
B	0.08	0.13	0.07	0.05	0.08	0.17	0.20	0.10	0.11	0.16	0.16	0.16	0.09	0.19	0.15

-: no data.

Unlike other elements, U is a radioactive element that can pollute the environment while serving as an important strategic resource [34,35]. The ML8 sample's U element enrichment coefficient is 13.78, indicating considerable enrichment. Sun et al. [31] proposed that the industrial index of recycling uranium content of raw coal is 40 μg/g, which is 20 times the global average. Therefore, the U content of ML8 (33.5 μg/g) is close to the industrial index of recycling (Figure 6).

The potentially hazardous trace elements in Shanxi coal include As, B, Ba, Cd, Cl, Co, Cr, Cu, F, Hg, Mn, Mo, Ni, Pb, Sb, Se, Th, U, V, and Zn [36]. As, Cl, F, Hg, and Se were not tested in this study. Pyrite nodules are the primary carriers of As and Se. The As content in Malan No. 8 coal pyrite nodule is 100 times that in most coal in China and 200 times that in Carboniferous–Permian coal in North China. Se content is more than 20 times that in most coal in China and that in C–P coal in North China [37]. Cu, Mo, Cd of ML8, Mo of DQ8, and Th of ZCD8 were identified as enrichment elements by this test. In some well fields, other elements are enriched. Sc and Ta of ZCD8, for example, are slightly enriched. Pb, Cr of BJZ9, Zn and Sn of GD9, XM9, and XQ9 are slightly enriched elements in No. 9 coal. The remaining elements, such as Li of DQ9 and Sn of XQ9, are slightly enriched (Tables 5 and 6).

When compared to No. 9 coal, Cr, Zn, Ga, Sr, Cd, In, Hf, Pb, P, Zr, Sn, and B of No. 8 coal are depleted, while other elements are relatively enriched, with a relative ratio of Cu, Mo, Cs, W, Bi, and U greater than 2 (Figure 8).

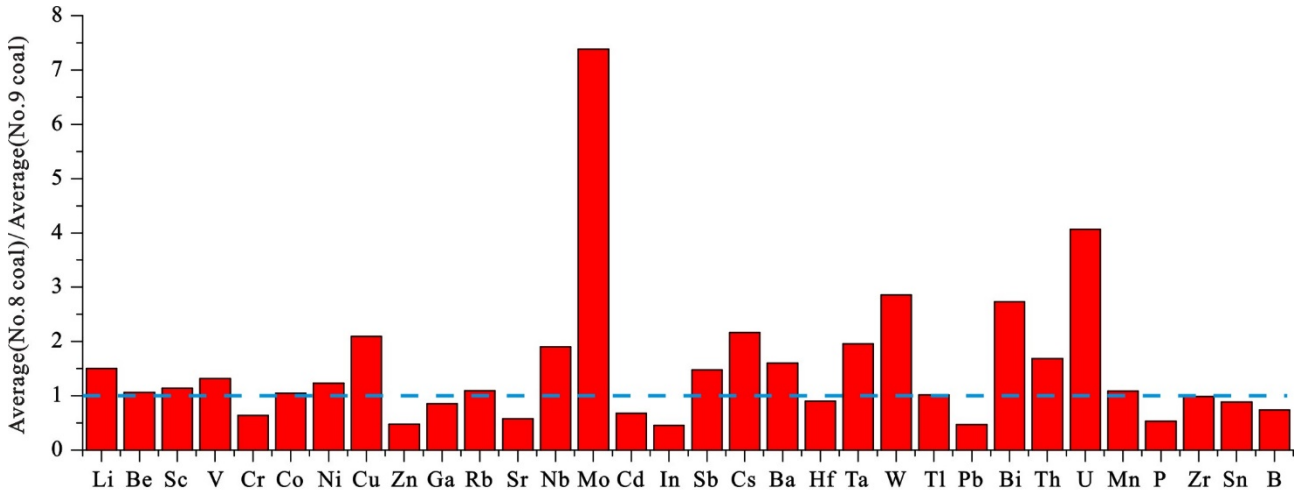

Figure 8. Average element content ratio of No. 8 coal and No. 9 coal.

4.4. Rare Earth Element

The total content of REY in No. 8 coal ranges from 17.65 to 98.51 μg/g, with an average of 60.74 μg/g. The content in the Baijiazhuang, Ximing, and Malan well fields are relatively low, and the content in the Tunlan, Duerping, and Dongqu well fields is relatively high (Figure 9). The total content of REY in No. 9 coal ranges from 41.93 to 165.80 μg/g, with an average of 75.55 μg/g, which is higher than that of No. 8 coal, similar to the distribution of No. 8 coal. The Dongqu well field has the highest content (165.80 μg/g), and it gradually decreases toward the west and east (Figure 10). The average content of REY in both coals are lower than that of Chinese coal (138 μg/g) [38] (Dai et al., 2016) (Table 7).

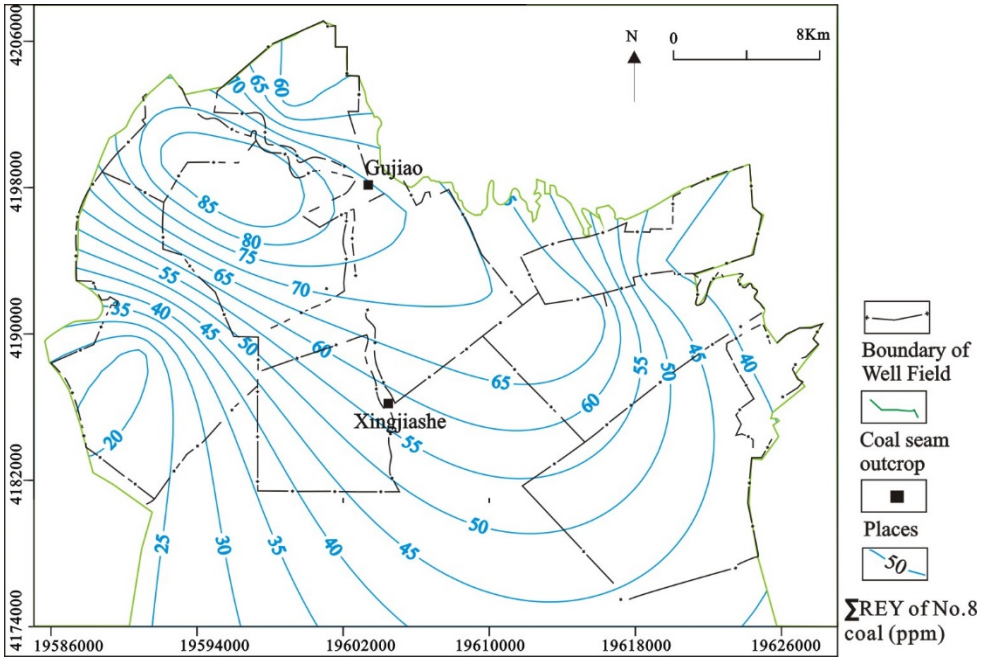

Figure 9. Total content of REY in No. 8 coal.

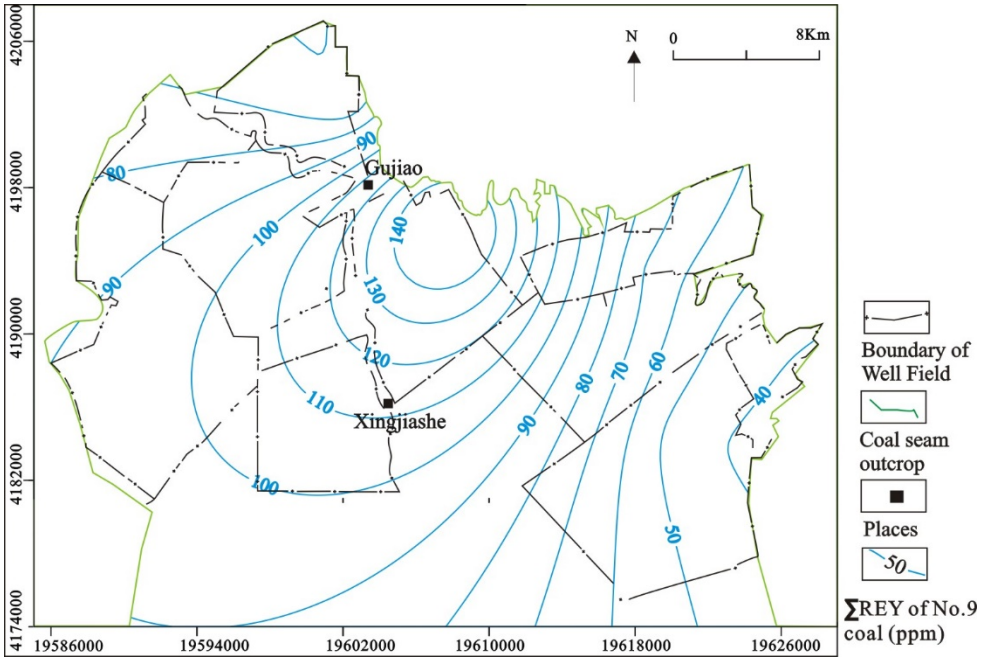

Figure 10. Total content of REY in No. 9 coal.

4.5. Occurrence of Trace Elements

We can gain a preliminary understanding of the occurrence states of trace elements and major elements using the correlation coefficient between elements [9]. Li, Sc, and Ba strongly correlate with Al, indicating that they are primarily enriched in aluminosilicate. No trace element has a strong correlation with Ca ($r > 7$), and Ga, Sr, and Mn have a weak correlation with Ca, indicating that some of them may occur in carbonate rocks. Cr, Ni, Tl, and Pb strongly correlate with Fe elements, implying that these elements are mostly found in sulfide (Table 8). The main occurrence form of Pb may be galena (PbS) with a different structure [40].

Table 7. Rare earth element content of coal samples (μg/g).

Sample	La	Ce	Pr	Nd	Sm	Eu	Gd	Tb	Dy	Y	Ho	Er	Tm	Yb	Lu	∑REY	Eu_N/Eu_N^*	Ce_N/Ce_N^*	La_N/Gd_N	La_N/Lu_N	Sm_N/Lu_N
BJZ8	9.60	14.09	1.42	4.55	0.72	0.12	0.69	0.11	0.63	4.16	0.13	0.37	0.07	0.41	0.07	37.12	0.85	0.84	1.10	1.47	2.01	0.83
DEP8	14.37	26.05	2.81	9.13	1.63	0.28	1.56	0.27	1.59	10.6	0.33	0.91	0.17	0.98	0.19	70.92	0.93	0.82	1.03	0.80	1.32	0.69
DQ8	15.36	31.62	3.09	9.54	1.60	0.32	1.65	0.25	1.29	8.91	0.23	0.59	0.10	0.52	0.11	75.17	1.04	0.98	1.13	1.55	1.44	1.31
ML8	2.81	4.96	0.61	2.14	0.46	0.11	0.50	0.10	0.69	4.10	0.14	0.40	0.08	0.44	0.11	17.65	0.86	0.98	0.94	0.28	0.91	0.39
TL8	29.68	40.07	3.95	12.42	1.70	0.28	1.55	0.22	1.13	5.97	0.21	0.57	0.10	0.55	0.13	98.51	0.81	0.88	1.16	2.35	2.62	0.97
XM8	7.38	14.31	1.67	5.64	1.01	0.16	0.98	0.18	1.06	6.41	0.21	0.60	0.12	0.64	0.13	40.47	0.93	0.74	1.00	0.60	1.10	0.63
XQ8	11.55	21.13	2.38	7.94	1.44	0.25	1.37	0.24	1.42	7.84	0.27	0.72	0.13	0.73	0.19	57.62	0.92	0.84	1.00	0.66	1.20	0.62
ZCD8	11.45	33.30	3.96	13.47	2.59	0.49	2.32	0.44	2.66	14.1	0.50	1.28	0.24	1.27	0.40	88.48	1.11	0.91	0.94	0.31	0.66	0.49
BJZ9	8.08	13.88	1.55	5.42	1.02	0.19	1.05	0.19	1.17	7.55	0.24	0.65	0.12	0.69	0.14	41.93	0.89	0.85	1.00	0.61	1.19	0.63
DQ9	29.46	59.44	8.08	34.10	9.19	1.61	4.78	0.47	2.14	13.0	0.42	1.22	0.23	1.28	0.36	165.80	0.88	1.13	1.08	0.88	0.48	1.13
GD9	8.92	13.56	1.40	4.80	1.03	0.18	0.99	0.19	1.27	7.90	0.26	0.72	0.14	0.79	0.18	42.32	0.86	0.79	0.94	0.54	1.30	0.47
XM9	11.96	22.21	2.75	9.88	1.71	0.28	1.78	0.33	1.94	11.2	0.38	1.05	0.20	1.12	0.23	67.02	0.88	0.76	1.00	0.55	1.05	0.64
XQ9	10.50	17.78	2.11	7.54	1.62	0.33	1.58	0.31	1.98	13.5	0.42	1.18	0.23	1.28	0.27	60.66	0.86	0.94	0.95	0.41	0.97	0.49

∑REY: total content of rare earth elements (∑REE = La + Ce + Pr + Nd + Sm + Eu + Gd + Tb + Dy + Y + Ho + Er + Tm + Yb + Lu); $Ce_N/Ce_N^* = Ce_N/(0.5La_N + 0.5Pr_N)$; $Eu_N/Eu_N^* = Eu_N/[(Sm_N \times 0.67) + (Tb_N \times 0.33)]$, where N refers to a UCC-normalized value. The upper continental crust (UCC) reported by Taylor and McLennan [39].

Table 8. The correlation coefficient distribution of major elements and trace elements.

The Range of Correlation Coefficient	Elements (Correlation Coefficient)
Al (Represents the affinity of aluminosilicate)	
$r > 0.7$	Li (0.84), Sc (0.70), Ba (0.74)
$0.5 \leq r \leq 0.69$	Nb (0.56), Hf (0.58), Ta (0.58), W (0.57), Bi (0.51), Th (0.59), Zr (0.59)
$0.35 \leq r \leq 0.49$	Cu (0.43), In (0.42)
Ca (Represents the affinity of carbonatite)	
$r > 0.7$	None
$0.5 \leq r \leq 0.69$	Ga (0.62), Sr (0.57), Mn (0.62)
$0.35 \leq r \leq 0.49$	Co (0.36), Pb (−0.35), B (−0.36)
Fe (Represents the affinity of sulphide)	
$r > 0.7$	Cr (0.86), Ni (0.75), Tl (0.78), Pb (0.70)
$0.5 \leq r \leq 0.69$	Co (0.57), Cd (0.54)
$0.35 \leq r \leq 0.49$	Be (0.48), Cu (0.46), Sr (−0.46), Mo (0.49), Sb (0.38), U (0.42), P (−0.49), Sn (−0.41)

4.6. Paleoenvironment

4.6.1. Paleosalinity

$K = (Fe_2O_3 + CaO + MgO)/(SiO_2 + Al_2O_3)$ can indicate the degree to which seawater or freshwater influences peat deposition. When K value ≤ 0.22, coal is primarily affected by freshwater during peat accumulation. When K value ≥ 0.23, coal is primarily affected by seawater [6,41]. The K value of No. 8 coal ranges from 0.03 to 0.54, with an average of 0.16, indicating a general trend of gradually increasing from northeast to southwest. The north is less affected by seawater, whereas the south is more affected (Figure 11a). The K value of No. 9 coal ranges from 0.02 to 0.95, with an average of 0.20, which is greater than 0.23 only near the Baijiazhuang well field in the east, indicating that the area in the east is more influenced by seawater (Figure 11b).

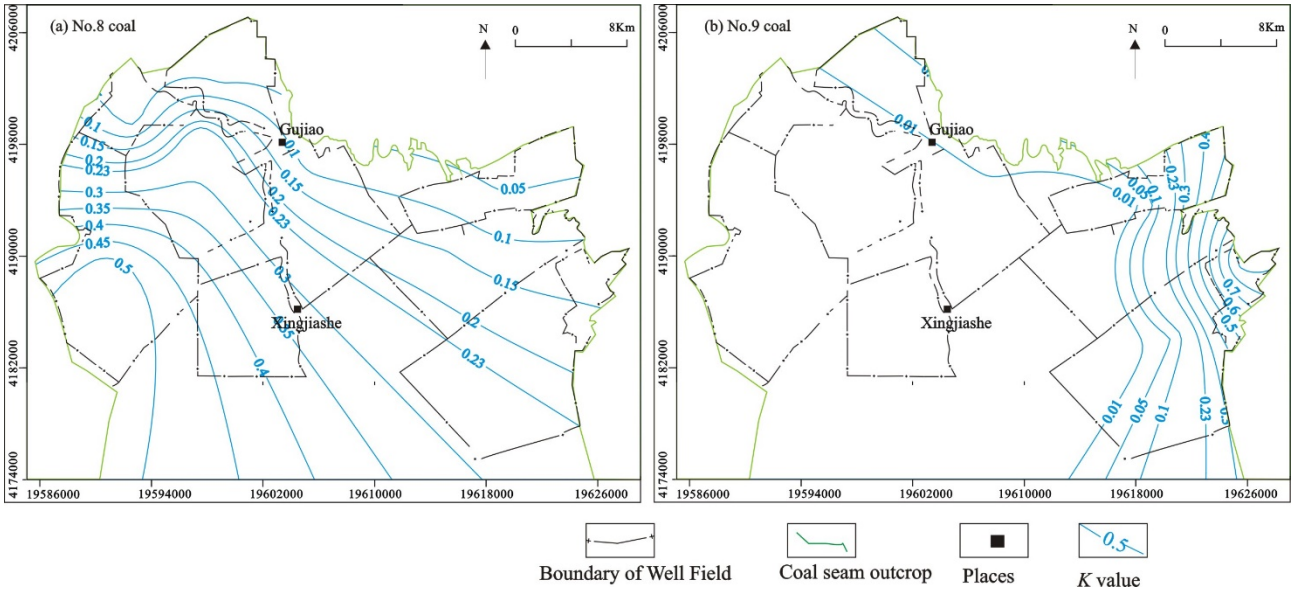

Figure 11. *K* value distribution of coal seams.

Coal's Sr/Ba ratio can indicate a sedimentary environment [42,43]. A Sr/Ba ratio greater than 1 indicates a marine sedimentary environment, and a ratio less than 1 indicates a continental sedimentary environment [44,45]. The Sr/Ba ratio of No. 8 coal ranges from 0.59 to 12.10, with an average of 3.39 (Table 9), indicating that it was formed in a marine sedimentary environment. The Tunlan well field has a higher ratio than that of the Malan, Zhenchengdi, Ximing, Duerping, and Guandi well fields (Figure 12a). The Sr/Ba ratio of No. 9 coal ranges from 1.13 to 12.51, with an average of 7.83, which is higher than the No. 8 coal ratio. Therefore, it represents the marine sedimentary environment. The Sr/Ba ratio of No. 9 coal is generally higher in the east of the study area, indicating that these areas are heavily influenced by seawater (Figure 12b). Based on the *K* value and Sr/Ba ratio, the influence of seawater on the south of No. 8 coal is greater than that on the north and the influence of seawater on the east of No. 9 coal is greater than that on the west.

Table 9. Element content ratio.

Samples	Sr/Ba	U/Th	Ni/Co	V/Cr
BJZ8	2.18	0.31	3.36	1.48
DEP8	2.80	0.23	1.30	2.41
DQ8	0.59	0.58	4.05	1.55
ML8	3.05	11.57	12.28	2.63
TL8	12.10	0.42	2.71	1.60
XM8	2.27	0.18	4.00	1.69
XQ8	3.08	0.20	1.66	1.54
ZCD8	1.03	0.11	3.98	1.46
Minimum	0.59	0.11	1.30	1.46
Maximum	12.10	11.57	12.28	2.63
Average	3.39	1.70	4.17	1.80
BJZ9	1.31	0.29	3.80	0.22
DQ9	4.02	0.23	5.92	2.26
GD9	12.00	0.55	2.13	2.38
XM9	12.51	0.24	2.18	1.74
XQ9	9.29	0.46	3.56	2.16
Minimum	1.31	0.23	2.13	0.22
Maximum	12.51	0.55	5.92	2.38
Average	7.83	0.36	3.52	1.75

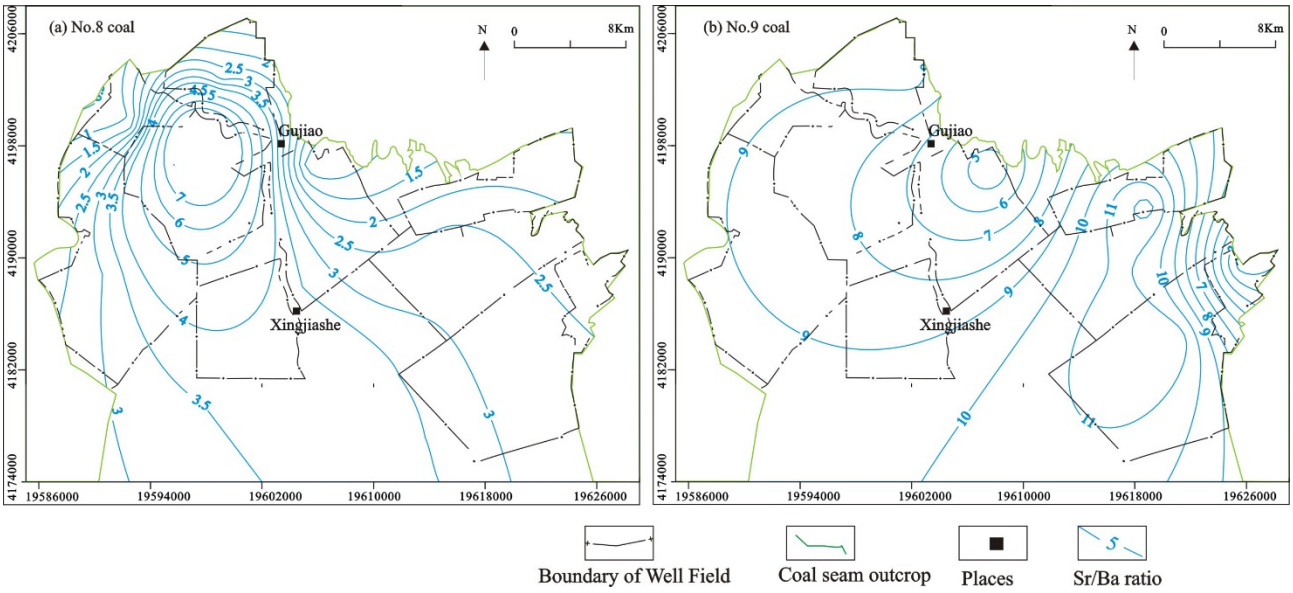

Figure 12. Sr/Ba ratio distribution of coal seams.

4.6.2. Redox Environment

No. 8 coal has a U/Th ratio ranging from 0.11 to 11.57, with an average of 1.70. Except for ML8 (11.57), the rest are less than 0.75. No. 8 coal has a Ni/Co ratio ranging from 1.30 to 12.28, with an average of 4.17. Except for ML8 (12.28), they are all less than 5, indicating an oxidation environment. The presence of ML8 coal indicates a reduction environment. No. 8 coal has a V/Cr ratio ranging from 1.46 to 2.63, with an average of 1.80. Except for DEP8 and ML8, the V/Cr ratio of the remaining samples is less than 2, indicating an oxidation environment. To summarize, except for the Malan well field, the coal-forming environment in most other areas is an oxidation environment.

The U/Th ratio of No. 9 coal ranges from 0.23 to 0.55, with an average of 0.36, indicating an oxidation environment. No. 9 coal has a Ni/Co ratio ranging from 2.13 to 5.92, with an average of 3.52. The rest of the samples are less than 5, indicating an oxidation environment, except for DQ9 (5.92), which is slightly greater than the critical value. No. 9 coal has a V/Cr ratio ranging from 0.22 to 2.38, with an average of 1.75. DQ9, GD9, and XQ9 have V/Cr ratios that are slightly higher than 2, indicating a suboxic to dysoxic environment. To summarize, No. 9 coal is formed through oxidation or suboxic to dysoxic environments (Tables 9 and 10).

Table 10. The discrimination index of redox environmental and corresponding parameters of samples [46].

Indicators	Redox Conditions			Parameters of Samples	
	Oxic	Suboxic to Dysoxic	Anoxic	No. 8 Coal	No. 9 Coal
U/Th	<0.75	0.75~1.25	>1.25	0.11~11.57	0.23~0.55
Ni/Co	<5.00	5.00~7.00	>7.00	1.30~12.28	2.13~5.92
V/Cr	<2.00	2.00~4.25	>4.25	1.46~2.63	0.22~2.38

4.7. Source Analysis

The Al_2O_3/TiO_2 ratio can be used to determine the sedimentary rock or coal seam source. Al_2O_3/TiO_2 ratios of 3–8, 8–21, and 21–70, respectively, indicate that the sediments are derived from mafic, intermediate, and felsic igneous rocks [47]. No. 8 coal has an Al_2O_3/TiO_2 ratio ranging from 16.09 to 354.47, with an average of 76.43. No. 9 coal has an Al_2O_3/TiO_2 ratio ranging from 39.79 to 88.64, with an average of 56.64. Two coal seams' sediment sources are primarily felsic igneous rocks (Table 2).

Rare earth elements and yttrium enrichments in coal are similar (Figure 13). Three enrichment types [8,48] are categorized as follows: L-type (light REY; $La_N/Lu_N > 1$), M-type (medium-REY; $La_N/Sm_N < 1$, $Gd_N/Lu_N > 1$), and H-type (heavy REY; $La_NLu_N < 1$). BJZ8, DQ8, and TL8 are L-type coal samples, and the remaining No. 8 coal samples are heavy rare earth element-based. The majority of No. 9 coal samples are H-type and DQ9 is M-type (Table 7).

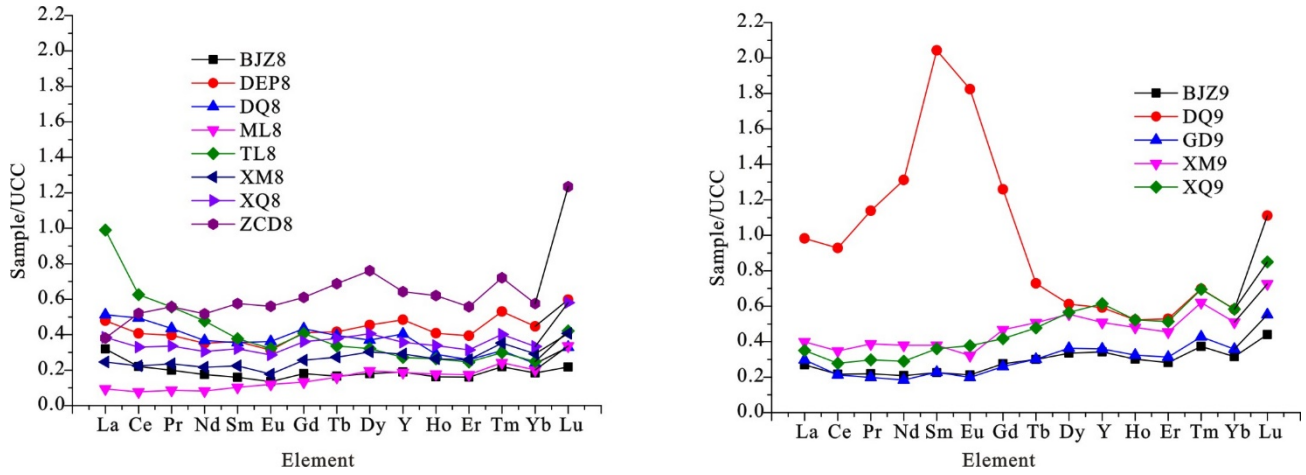

Figure 13. Chondrite-normalized REE patterns of coal samples.

To understand the influence of Ba on Eu content in ICP–MS experiments, the Ba/Eu ratios of 8 and 9 coal are calculated to be less than 1000, allowing the influence of Ba on Eu to be ignored [49]. The Eu_N/Eu_N^* values of the No. 8 coal seam range from 0.74 to 0.98, with an average of 0.87 indicating a weak relationship. The most obvious negative anomalies are those of XM8; Eu_N/Eu_N^* values of No. 9 coal seam range from 0.76 to 1.13, with an average of 0.90. Except for DQ9, Eu elements exhibit only minor negative anomalies. In general, a negative Eu anomaly indicates that the sediment source is felsic rock, the coal seam is preserved within carbonate successions and the temperature affected by the hydrothermal fluid is less than 200 °C. The source indication is consistent with the Al_2O_3/TiO_2 ratio. The Ce_N/Ce_N^* values of No. 8 coal range from 0.81 to 1.11, with an average of 0.93, and those of No. 9 coal seam range from 0.86 to 0.89, with an average of 0.87. ZCD8 and DQ8 both show slightly positive anomalies, and the rest are negative anomalies, indicating that the origin of coal seams are primarily terrigenous materials formed in a marine-influenced environment [38]. The Carboniferous–Permian sediments in the Xishan coalfield are derived from the Inner Mongolia Uplift on North China's northern margin [50], which is consistent with the negative Ce element anomaly.

5. Conclusions

No. 8 and No. 9 coal from nine mines in the study area were sampled and tested to understand the specific area of enrichment element and the changing trend of the sedimentary environment in the middle and north of Xishan coalfield. The characteristics of the coal's quality, element occurrence, enrichment, and sedimentary environment were investigated. The following conclusions have been drawn:

(1) The major elements in No. 8 and No. 9 coal ashes are Si and Al, followed by Ca and Fe. The minerals found in coal are primarily kaolinite. Quartz, pyrite, and calcite were found in some samples.

(2) Li and U are enriched elements in No. 8 coal. Li in the study area has a general decreasing trend from northwest to southeast and a rapidly decreasing trend in the northwest. The U enrichment coefficient of ML8 is 13.78, which is close to the industrial index of recycling. Enrichment hazardous trace elements include Cu, Mo, Cd of ML8, Mo of DQ8, and Th of ZCD8. The elements Li of DQ9, Pb and Cr of BJZ9,

Zn and Sn of GD9, XM9, and XQ9 are slightly enriched. The elements Li, Sc, and Ba strongly correlate with Al, indicating that they are primarily rich in aluminosilicate. Cr, Ni, Tl, and Pb strongly correlate with Fe, implying that these elements are primarily found in sulfide.

(3) The total content of REY in No. 8 coal is low in the Baijiazhuang, Ximing, and Malan well fields and high in the Tunlan, Duerping, and Dongqu well fields. The total REY content of No. 9 coal is the highest in the Dongqu well field, gradually decreasing to the west and east. BJZ8, DQ8, and TL8 are L-type coal samples, and the remaining No. 8 coal samples are heavy rare earth element types. The majority of NO. 9 coal samples are H-type and DQ9 is M-type.

(4) Based on *K* value and Sr/Ba ratio, seawater has a greater influence on deposition of No. 8 coal to the south of than to the north. The influence of seawater on the deposition of No. 9 coal is greater in the east than in the west. No. 8 coal (except ML8) is formed in an oxidation environment, and ML8 coal is formed in a reduction environment, based on the U/Th, Ni/Co, and V/Cr ratios. The oxidation or suboxic to the dysoxic environment resulted in the formation of No. 9 coal.

(5) Based on the Al_2O_3/TiO_2 ratio, Eu_N/Eu_N^*, and Ce_N/Ce_N^* anomalies, it is assumed that the No. 8 and No. 9 coal sediments primarily comprise felsic igneous rocks. The provenance area is similar, originating primarily from the Inner Mongolia Uplift on North China's northern margin.

Author Contributions: G.W. wrote the paper, conducted the experimental study, analyzed the results; Y.Q. contributed to experimental study; Y.X. contributed to sample collection and preparation. All authors have read and agreed to the published version of the manuscript.

Funding: This work was supported by the Key Project of Natural Science Foundation of China under Grant No. 530314.

Conflicts of Interest: The authors declare no conflict of interest.

References

1. Wu, P.; Li, J.; Zhuang, X.; Querol, X.; Moreno, N.; Li, B.; Ge, D.; Zhao, S.; Ma, X.; Cordoba, P.; et al. Mineralogical and Environmental Geochemistry of Coal Combustion Products from Shenhuo and Yihua Power Plants in Xinjiang Autonomous Region, Northwest China. *Minerals* **2019**, *9*, 496. [CrossRef]
2. Yao, Z.T.; Ji, X.S.; Sarker, P.K.; Tang, J.H.; Ge, L.Q.; Xia, M.S.; Xi, Y.Q. A comprehensive review on the applications of coal fly ash. *Earth Sci. Rev.* **2015**, *141*, 105–121. [CrossRef]
3. Munawer, M.E. Human health and environmental impacts of coal combustion and post-combustion wastes. *J. Sustain. Min.* **2017**, *17*, 887–896.
4. Finkelman, R.B.; Tian, L.W. The health impacts of coal use in china. *Int. Geol. Rev.* **2018**, *60*, 579–589. [CrossRef]
5. Liu, Y.; Liu, G.; Yousaf, B.; Zhou, C.; Shen, X. Identification of the featured-element in fine road dust of cities with coal contamination by geochemical investigation and isotopic monitoring. *Environ. Int.* **2021**, *152*, 106499. [CrossRef]
6. Zheng, Q.; Shi, S.; Liu, Q.; Xu, Z. Modes of occurrences of major and trace elements in coals from Yangquan mining district, north china. *J. Geochem. Explor.* **2017**, *175*, 36–47. [CrossRef]
7. Xie, P.; Hower, J.C.; Nechaev, V.P.; Ju, D.; Liu, X. Lithium and redox-sensitive (Ge, U, Mo, V) element mineralization in the Pennsylvanian coals from the Huangtupo coalfield, Shanxi, northern China: With emphasis on the interaction of infiltrating seawater and exfiltrating groundwater. *Fuel* **2021**, *300*, 120948. [CrossRef]
8. Seredin, V.V.; Dai, S. Coal deposits as potential alternative sources for lanthanides and yttrium. *Int. J. Coal Geol.* **2012**, *94*, 67–93. [CrossRef]
9. Yang, N.; Tang, S.; Zhang, S.; Xi, Z.; Li, J.; Yuan, Y.; Guo, Y. In seam variation of element-oxides and trace elements in coal from the eastern Ordos basin, China. *Int. J. Coal Geol.* **2018**, *197*, 31–41. [CrossRef]
10. Liu, H.; Ma, Z.; Guo, Y.; Cheng, F. Occurrence characteristics and industrial prospects of lithium and gallium in coal in Taiyuan Xishan coalfield. *Clean Coal Technol.* **2018**, *24*, 30–36. (In Chinese with English Abstract)
11. Liu, D.; Zeng, F.; Zhao, F.; Wang, D.; Xie, X.; Zou, Y. Status and prospect of research for three type coal-associated rare earth resources in coal measures in Shanxi province. *Coal Geol. Explor.* **2018**, *46*, 1–7. (In Chinese with English Abstract)
12. Sun, B.; Zeng, F.; Li, F.; Qi, F. Geochemistry characteristics of trace elements & rare earth elements (REEs) of No. 8 coal and parting in Malan Coal Mine, Xishan Coalfield. J. *China Coal Soc.* **2010**, *35*, 110–116. (In Chinese with English Abstract)
13. Zhen, L. *Geochemistry of No.8 Coal and Its Relationship with Coal Metamorphism in Xishan Coalfield, Taiyuan*; Taiyuan University of Technology: Taiyuan, China, 2014. (In Chinese with English Abstract)

14. Yang, J. Relationship between lanthanides and organic matter in coal from FTIR analysis results: An example of No. 8 coal seam from Taiyuan Xishan Mine, North China. *J. China Coal Soc.* **2015**, *40*, 1109–1116. (In Chinese with English Abstract)
15. Wang, J.; Chen, L.; Wu, W.; Hu, L.; Zhang, B.; Liao, J. Geochemical Characteristics and Geological Significance of Trace Elements in Xishan Coalfield, Taiyuan. *Sci. Technol. Eng.* **2016**, *16*, 15–21. (In Chinese with English Abstract)
16. Zhao, L.; Qin, Y.; Cai, C.; Xie, Y.; Wang, G.; Huang, B.; Xu, C. Control of coal facies to adsorption-desorption divergence of coals: A case from the Xiqu drainage area, Gujiao CBM block, north china. *Int. J. Coal Geol.* **2017**, *171*, 169–184. [CrossRef]
17. Sun, F. Occurrence regularity of lithium in No.8 coal seam of Gujiao Mining Area in Xishan coalfield. *Coal Sci. Technol.* **2018**, *46*, 202–207. (In Chinese with English Abstract)
18. Zhang, H. *Study on the Characteristics of elements and PAHs of Coal Gangue of Duerping Coal Deposit*; Taiyuan University of Technology: Taiyuan, China, 2012. (In Chinese with English Abstract)
19. Pu, W.; Sun, B.; Li, Z.; Li, M.; Yang, G.; Zeng, F. Geochemistry of trace and rare elements in No.2 coalseam parting in Malan coal mine and its geological implication. *J. China Coal Soc.* **2012**, *37*, 1709–1716. (In Chinese with English Abstract)
20. Wang, G.; Xie, Y.; Qin, Y.; Wang, J.; Shen, J.; Han, B.; Liang, C.; Wang, Q. Element geochemical characteristics and formation environment for the roof, floor and gangue of coal seams in the Gujiao mining area, Xishan coalfield, China. *J. Geochem. Explor.* **2018**, *190*, 336–344. [CrossRef]
21. Sun, B.; Zeng, F.; Li, X.; Liu, C. Time of coal rank formation for Ximing-Duerping mining area inXishan coalfield, Taiyuan: Evidence from zircon fission track dating. *J. China Coal Soc.* **2013**, *38*, 2023–2029. (In Chinese with English Abstract)
22. Wang, G.; Qin, Y.; Xie, Y.; Shen, J.; Zhao, L.; Huang, B.; Zhao, W. Coalbed methane system potential evaluation and favourable area prediction of gujiao blocks, xishan coalfield, based on multi-level fuzzy mathematical analysis. *J. Pet. Sci. Eng.* **2018**, *160*, 136–151. [CrossRef]
23. Taylor, G.H.; Teichmüller, M.; Davis, A.; Diessel, C.F.K.; Littke, R.; Robert, P. *Organic Petrology*; Gebrüder Borntraeger: Berlin, Germany, 1998; 704p.
24. International Committee for Coal and Organic Petrology (ICCP). The new vitrinite classification (ICCP System 1994). *Fuel* **1998**, *77*, 349–358. [CrossRef]
25. International Committee for Coal and Organic Petrology (ICCP). The new inertinite classification (ICCP System 1994). *Fuel* **2001**, *80*, 459–471. [CrossRef]
26. Dai, S.; Wang, X.; Zhou, Y.; Hower, J.C.; Li, D.; Chen, W.; Zhu, X. Chemical and mineralogical compositions of silicic, mafic, and alkali tonsteins in the Late Permian coals from the Songzao Coalfield, Chongqing. Southwest China. *Chem. Geol.* **2011**, *282*, 29–44. [CrossRef]
27. Dai, S.; Zhang, W.; Seredin, V.V.; Ward, C.R.; Hower, J.C.; Song, W.; Wang, X.; Li, X.; Zhao, L.; Kang, H.; et al. Factors controlling geochemical and mineralogical compositions of coals preserved within marine carbonate successions: A case study from the heshan coalfield, southern china. *Int. J. Coal Geol.* **2013**, *109*, 77–100. [CrossRef]
28. Yuan, Y.; Tang, S.; Zhang, S. Geochemical and Mineralogical Characteristics of the Middle Jurassic Coals from the Tongjialiang Mine in the Northern Datong Coalfield, Shanxi Province, China. *Minerals* **2019**, *9*, 184. [CrossRef]
29. Dai, S.; Ren, D.; Tang, Y. Modes of occurrence of major elements in coal and their study significance. *Coal Geol. Explor.* **2005**, *33*, 1–5. (In Chinese with English Abstract)
30. Li, B.; Zhuang, X.; Li, J.; Querol, X.; Font, O.; Moreno, N. Enrichment and distribution of elements in the late Permian coals from the Zhina coalfield, Guizhou province, southwest china. *Int. J. Coal Geol.* **2017**, *171*, 111–129. [CrossRef]
31. Sun, Y.; Zhao, C.; Li, Y.; Wang, J. Minimum mining grade of the selected trace elements in Chinese coal. *J. China Coal Soc.* **2014**, *39*, 744–748. (In Chinese with English Abstract)
32. Dai, S.; Ren, D.; Chou, C.L.; Finkelman, R.B.; Seredin, V.V.; Zhou, Y. Geochemistry of trace elements in Chinese coals: A review of abundances, genetic types, impacts on human health, and industrial utilization. *Int. J. Coal Geol.* **2012**, *94*, 3–21. [CrossRef]
33. Ren, D.; Zhao, F.; Dai, S. *Geochemistry of Trace Elementsin Coal*; Science Press: Beijing, China, 2006; pp. 82–83. (In Chinese)
34. Duan, P.; Wang, W.; Sang, S.; Qian, F.; Shao, P.; Zhao, X. Partitioning of hazardous elements during preparation of high uranium coal from rongyang, Guizhou, China. *J. Geochem. Explor.* **2018**, *185*, 81–92. [CrossRef]
35. Dai, S.; Finkelman, R.B. Coal as a promising source of critical elements: Progress and future prospects. *Int. J. Coal Geol.* **2018**, *186*, 155–164. [CrossRef]
36. Zhang, J.; Zheng, C.; Ren, D.; Chou, C.; Liu, J.; Zeng, R.; Wang, Z.; Zhao, F.; Ge, Y. Distribution of potentially hazardous trace elements in coals from Shanxi province, China. *Fuel* **2004**, *83*, 129–135. [CrossRef]
37. Sun, R.; Liu, G.; Zheng, L.; Chou, C. Geochemistry of trace elements in coals from the Zhuji mine, Huainan coalfield, Anhui, China. *Int. J. Coal Geol.* **2010**, *81*, 81–96. [CrossRef]
38. Dai, S.; Graham, I.T.; Ward, C.R. A review of anomalous rare earth elements and yttrium in coal. *Int. J. Coal Geology* **2016**, *159*, 82–95. [CrossRef]
39. Taylor, S.R.; McLennan, S.H. *The Continental Crust: Its Composition and Evolution*; Blackwell: Oxford, UK, 1985; p. 312.
40. Finkelman, R.B. Modes of occurrence of potentially hazardous elements in coal: Levels of confidence. *Fuel Process. Technol.* **1994**, *39*, 21–34. [CrossRef]
41. Qin, S.; Gao, K.; Sun, Y.; Wang, J.; Zhao, C.; Li, S.; Lu, Q. Geochemical characteristics of rare-metal, rare-scattered, and rare-earth elements and minerals in the late Permian coals from the moxinpo mine, Chongqing, china. *Energy Fuels* **2018**, *32*, 3138–3151. [CrossRef]

42. Leila, M.; Moscariello, A.; Šegvić, B. Geochemical constraints on the provenance and depositional environment of the Messinian sediments, onshore Nile Delta, Egypt: Implications for the late Miocene paleogeography of the Mediterranean. *J. Afr. Earth Sci.* **2018**, *143*, 215–241. [CrossRef]
43. Meng, Q.T.; Liu, Z.J.; Bruch, A.A.; Liu, R.; Hu, F. Palaeoclimatic evolution during Eocene and its influence on oil shale mineralization, Fushun basin, China. *J. Asian Earth Sci.* **2012**, *45*, 95–105. [CrossRef]
44. Zhang, S.; Liu, C.; Liang, H.; Wang, J.; Bai, J.; Yang, M.; Liu, G.; Huang, H.; Guan, Y. Paleoenvironmental conditions, organic matter accumulation, and unconventional hydrocarbon potential for the Permian Lucaogou Formation organic-rich rocks in Santanghu Basin, NW China. *Int. J. Coal Geol.* **2018**, *185*, 44–60. [CrossRef]
45. Dai, S.; Bechtel, A.; Eble, C.F.; Flores, R.M.; French, D.; Graham, I.T.; Hood, M.M.; Hower, J.C.; Korasidis, V.A.; Moore, T.A.; et al. Recognition of peat depositional environments in coal: A review. *Int. J. Coal Geol.* **2020**, *219*, 1–67.
46. Jones, B.; Manning, D.A. Comparison of geochemical indices used for the interpretation of palaeoredox conditions in ancient mudstones. *Chem. Geol.* **1994**, *111*, 111–129. [CrossRef]
47. Dai, S.; Li, T.; Jiang, Y.; Ward, C.R.; Hower, J.C.; Sun, J.; Liu, J.; Song, H.; Wei, J.; Li, Q.; et al. Mineralogical and geochemical compositions of the pennsylvanian coal in the hailiushu mine, daqingshan coalfield, inner mongolia, China: Implications of sediment-source region and acid hydrothermal solutions. *Int. J. Coal Geol.* **2015**, *137*, 92–110. [CrossRef]
48. Dai, S.; Luo, Y.; Seredin, V.V.; Ward, C.R.; Hower, J.C.; Zhao, L.; Liu, S.; Zhao, C.; Tian, H.; Zou, J. Revisiting the late Permian coal from the Huayingshan, Sichuan, southwestern China: Enrichment and occurrence modes of minerals and trace elements. *Int. J. Coal Geol.* **2014**, *122*, 110–128. [CrossRef]
49. Yan, X.; Dai, S.; Graham, I.T.; He, X.; Shan, K.; Liu, X. Determination of Eu concentrations in coal, fly ash and sedimentary rocks using a cation exchange resin and inductively coupled plasma mass spectrometry (ICP-MS). *Int. J. Coal Geol.* **2018**, *191*, 152–156. [CrossRef]
50. Wu, J.; Sun, B.; Liu, C.; Zeng, F. The Provenance Analysis of Taiyuan Formation Sandstone in the Xishan Coal Field, Taiyuan. *Sci. Technol. Eng.* **2016**, *16*, 102–107. (In Chinese with English Abstract)